RESEARCH Open Access

Analyzing voltage stability challenges under high photovoltaic penetration in Niger' s electrical grid

Hamza Abarchi Halarou[1*], Yacouba Moumouni[2†], Bonkaney Abdou Latif[3†], Andrea Benigni[4†] and Madougou Saidou[3†]

†Yacouba Moumouni, Bonkaney Abdou Latif, Andrea Benigni, and Madougou Saidou contributed equally to this work.

*Correspondence:
Hamza Abarchi Halarou
halarouhzab@gmail.com
[1]Doctoral Research Program in Climate Change and Energy (DRP-CCE), West African Science Service Centre on Climate Change and Adapted Land Use (WASCAL), RN6, Niamey 10896, Niger
[2]Electrical and Electronics Engineering, Higher Colleges of Technology, Ras Al Khaimah Women's College, Sultan Al Kabeer street, Ras Al Khaimah 4792, United Arab Emirates
[3]Department of Physics, Ecole Normale Superieure, Abdou Moumouni University, RN6, Niamey 10896, Niger
[4]Institute of Climate and Energy Systems (ICE-1), Forschungszentrum Juelich, Wilhelm-Johnen Street, Juelich 52428, Germany

Abstract
The integration of solar photovoltaic (PV) power plants into the electricity grid offers a sustainable solution to meet rising energy demand, particularly in regions with abundant solar resources like Niger. However, high PV penetration introduces challenges to grid stability, including voltage fluctuations, increased power losses, and line overloading. This study investigates the impact of substantial PV integration on the voltage stability of the Nigerien River Zone (RZ) grid, which accounts for approximately 68% of the country's total energy consumption. Using quasi-dynamic simulations, the study examines grid performance across three selected months, viz., January, May, and August, to capture both daily and seasonal variations in demand and PV generation. Results reveal that periods characterized by peak demand and diminished PV output exhibited the most pronounced grid stress, with significant voltage deviations, increased power losses, and marked changes in the Voltage Stability Index (VSI). In August, frequent cloud cover leads to intermittent PV generation and increased variability, whereas May demonstrates relatively stable conditions during early afternoon hours. Key challenges include voltage instability during high demand, persistent overloading of major transmission lines, and heightened power loss linked to renewable variability. Recommendations include targeted interventions such as grid reinforcements, advanced reactive power support, energy storage systems deployment, and demand-side management strategies to enhance grid reliability. This study provides novel insights into the dual challenges of high demand and renewable variability, offering practical guidance to support Niger's transition to sustainable and resilient energy system.

Keywords Niger, Photovoltaic penetration, Power losses, Quasi-dynamic simulations, Stability index, Voltage stability

1 Introduction

The global transition to renewable energy, particularly solar photovoltaic (PV), continues to gain traction as part of a more sustainable energy future [1]. While this shift offers clean energy and the potential for lower operational cost, it also presents technical challenges, notably, preserving voltage stability under high penetration levels of intermittent generation. Such challenges are amplified in developing countries, where grids often lack robust infrastructure to accommodate rapid fluctuation in generation and load [2].

In Niger, despite having immense solar potential, the power infrastructure remains underdeveloped [3], making the grid susceptible to voltage disturbances as large-scale PV system are added. The River Zone (RZ), in particular, is experiencing growing electricity demand due to population expansion and urbanization [4]. Although expanding PV generation in the RZ can reduce fossil-fuel dependence and electricity imports, high PV penetration can lead to serious voltage regulation problems [5]. Variable solar outputs, exacerbated by cloud transients, can cause voltage fluctuations, reactive power imbalances, and even voltage instability [6]. Given that a 30 MW PV plant has already been integrated at Gorou Banda in 2023 and more PV projects are underway, there is an urgent need for a rigorous, data-driven analysis of how these additions will affect the grid's voltage profile stability. Voltage stability refers to the power system's capacity to maintain acceptable voltage levels under normal conditions and after being subjected to disturbances such as variation in load or generation [7]. Traditionally, synchronous generators inherently provide voltage support through reactive power. In contrast, PV installations use power-electronics-based interfaces, often operating under maximum power point tracking (MPPT) to optimize active power injection rather than providing significant reactive power support [8]. Rapid fluctuations in solar output, combined with low-inertia or weak grids, can induce voltage dips, overvoltage, or oscillations [9, 10]. Studies have shown that when PV penetration exceeds 30% of grid capacity, voltage swings can become more frequent and severe, requiring faster, more sophisticated control strategies than classical tap-changing transformers or manual capacitor switching [11, 12]. Indeed, issues of reverse power flow and voltage rise can stress local infrastructures, pushing voltages beyond permissible limits [13, 14].

The sensitivity of voltage stability to PV deployment also depends on grid topology and strength. Weaker grids, characterized by lower short-circuit ratios, have less capacity to dampen voltage deviations [15]. In such cases, even modest changes in generation or load can cause pronounced voltage instability, especially in areas far from load centers [16]. To counter these challenges, advanced inverter functionalities and grid support algorithms have been proposed. For instance, reactive power control, volt-VAR optimization, and fast voltage regulation can improve stability in systems with large PV shares [17]. A prominent example from the National Renewable Energy Laboratory (NREL) demonstrated that 300 MW of PV added to the Hawaiian Electric grid introduced significant voltage stability concerns; these were mitigated using advanced inverter stings such as dynamic reactive power injections and active power curtailment to actively smooth voltage fluctuations [18].

Despite extensive global research on voltage stability impacts of PV power plants, knowledge gaps persist regarding the unique conditions of developing grids like Niger?s RZ, where weak infrastructure, geographically distributed demand, and rapid load growth magnify instability risks. Moreover, the lack of localized studies makes it difficult to adopt generic solutions from well-developed systems elsewhere. Therefore, this paper seeks to bridge this gap by 1) evaluating how high penetration of PV affects the voltage stability in the Nigerien RZ grid using a comprehensive quasi-dynamic simulation framework, 2) introducing a voltage stability index (VSI) and total voltage distortion (TVD) metric to quantify the severity of voltage excursions under different operating conditions and, 3) proposing control strategies to mitigate adverse impacts, ensuring stable and reliable grid operation.

By integrating these innovative metrics (VSI, TVD) with real RZ grid data, this study not only provides new insights into PV integration challenges specific to Niger but also lays out practical recommendation for grid reinforcement and control solutions. The rest of the paper is organized as follow: section 2 details the study area, introduces the mathematical formulations of the voltages stability index and total voltage distortion, and quasi-dynamic simulation approach; section 3 presents the results and discussion, offering an in-depth analysis of observed voltage profiles and the efficacy of proposed mitigation strategies; finally, section 4 provides the conclusion and future research directions, highlighting how the findings can guide policy and technical decisions for sustainable, reliable PV integration in Niger and other similar contexts.

2 Methodology

2.1 Study area

The study area covers Niger's electricity network (Fig. 1), which is currently managed by "La Société Nigérienne d'Electricité (NIGELEC)". Since its establishment in 1968, NIGELEC has been solely responsible for electricity imports, local production, transmission, and distribution. The electricity system operated by NIGELEC is divided into four main zones, excluding isolated and border centers, corresponding to Niger's eight regions: 1) the River Zone, 2) the North-Centre-East Zone, 3) the North Zone, and 4) the East Zone [19]. However, these zones are not electrically interconnected, each zone operates independently with its own local generation, transmission, and distribution infrastructure.

This structural separation eliminate inter-zonal electrical interactions, justifying the modeling of the RZ in isolation. The RZ is the most densely populated and industrialized,

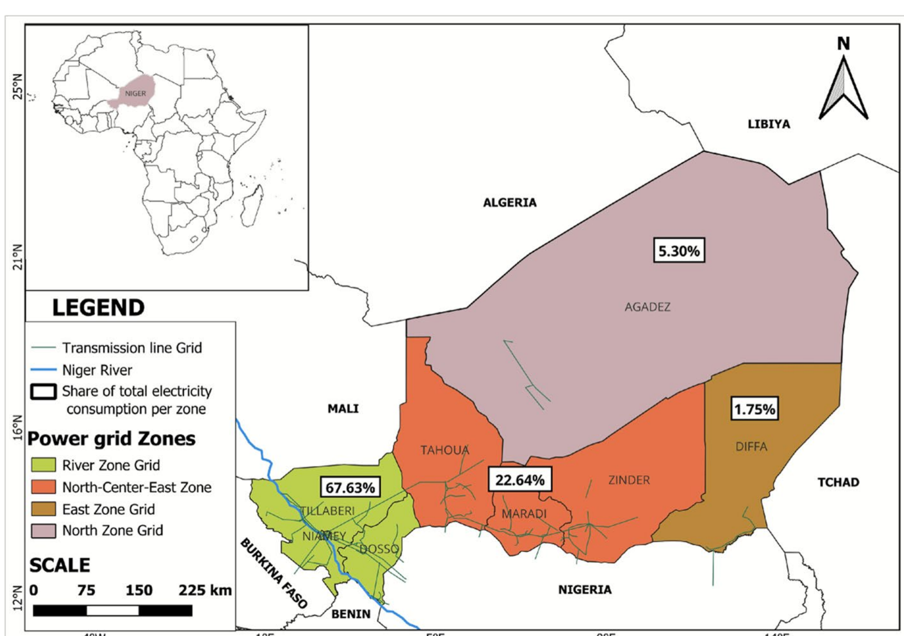

Fig. 1 Map of Niger and the associated electrical Zones [4]

Table 1 Installed generation capacity in RZ Grid (source: NIGELEC)

River zone grid		Capacity
Import from Nigeria	Contractual Power	120 MW
	Available power	65 MW
RZ Installed Capacity	Goudel Thermal plant	89 MW
	Gorou Banda Thermal Plant	100 MW
	Gorou Banda Solar PV Plant	30 MW

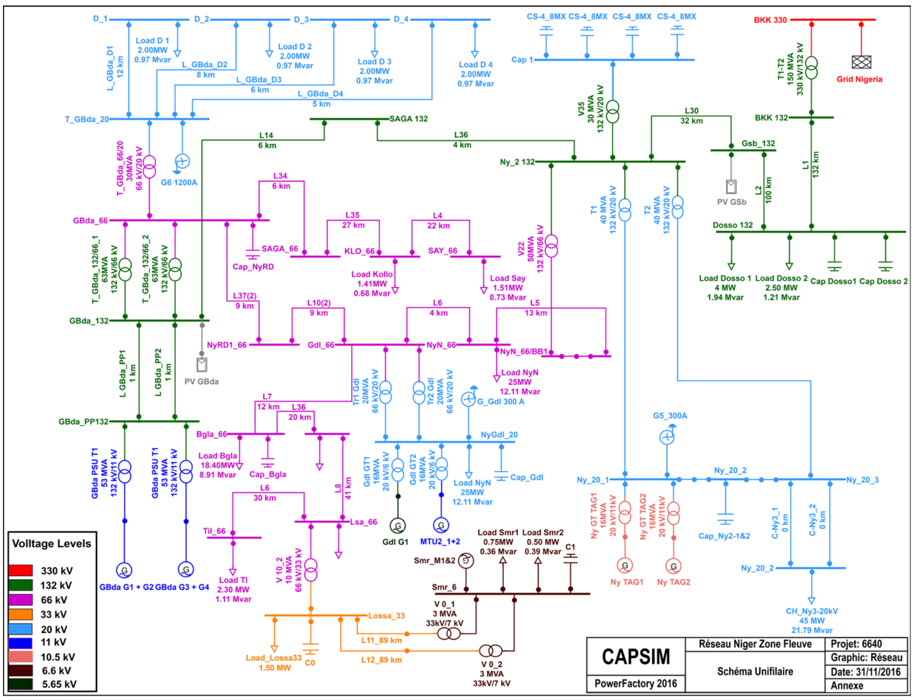

Fig. 2 Single-line diagram of the river zone power system [21]

accounting for a approximately 68% [4] of total energy consumption. This area encompasses the country's far western and southwestern parts, including the Niamey conurbation and the regions of Dosso and Tillabéry. The RZ grid region exhibits the country's greatest population density and the highest concentration of professional and economic activities. The western region is served by the 132kV Birnin-Kebbi interconnection line from Nigeria, which has a contractual capacity of 120MW, along with three power stations located at Goudel (thermal) and Gorou Banda (thermal and solar PV) [19, 20]. Table 1 presents a summary of the capacity of each plant. The RZ was selected for this study due to its significance in energy demand and the concentration of future solar and hydroelectric power plant projects in the region.

The network architecture is based on the single-line diagram developed by FICHTNER, which served as the structural reference for the River Zone model (see Fig. 2) [21]. This baseline configuration was implemented in Pandapower and subsequently updated to reflect the commissioning of major generation assets such as the Gorou Banda diesel plant and new PV installations. These updates ensure that the simulated network accurately represents the current operational state of the grid. Further details on these commissioning adjustments and data sources are provided in the following Data section.

2.2 Data

The River Zone (RZ) network relies on two critical transformation substations: the Dosso substation, which primarily serves the city of Dosso and nearby towns, and the Niamey II substation, which supports Niamey and its surroundings and houses the interconnection to the Nigerian grid [22]. While NIGELEC lacks the necessary asset for monitoring all the data of the system to provide a complete overview of the grid's electrical conditions, measuring devices have been installed at key locations, including Nigeria, Dosso, and the primary substation in Niamey. These devices record voltage and power data at an hourly resolution. The dataset spans from 2016 to 2023 and has been analyzed to understand the variation in load profiles and voltage levels across the network. In addition to historical data, information on planned infrastructure upgrades has been gathered to account for future enhancements to the RZ transmission system. Key projects include the 1) construction of a 132 kV double-circuit transmission line to transport power from the Kandadji Hydroelectric Station, 2) Reinforcement of the Niamey North power station to improve system reliability, 3) upgrading the Goudel's Niamey North line from 66 kV to 132 kV as well as the 4) replacement of aging transformers in Niamey II to enhance power flow efficiency. Plans also include integrating new solar power plants by 2028, with a breakdown of their capacities shown in Table 2.

2.3 Methods

The River Zone (RZ) electrical grid is modeled using the Pandapower tool-based Python. This open-source tool is widely used for electrical network modeling and analysis, enabling power flow simulation, short circuit analysis, and optimal power dispatch in distribution and transmission systems. In this study, we adopt a structured three-step methodology, as illustrated in Fig. 3, to assess voltage stability under high photovoltaic (PV) penetration. In the first step, we gather and preprocess technical grid data, including hourly voltage and load profiles across the year. In the second step, the RZ network is modeled with full AC power flow using Pandapower, and a quasi-dynamic simulation is conducted by injecting hourly time-series data. Key indicators such as voltage deviation, line loading, voltage stability index (VSI), and power losses are computed at each time step. The third step involves analyzing these results to determine how PV injection impacts system stability, reliability, and capacity limits. This workflow enables a detailed temporal assessment of grid behavior and the effectiveness of control strategies under realistic operating conditions [23, 24].

2.3.1 Network modelling in Pandapower

To investigate the impact of high PV penetration on the RZ electrical grid, we developed a detailed python-based Pandapower model. Pandapower provides an open-source environment for power flow, short-circuit analysis, and optimal power dispatch in both distribution and transmission systems [23, 24]. The network model was constructed

Table 2 Summary of the PV plant integration capacity in the RZ grid

PV plants	Capacity	Starting period	Source
Gorou Banda PV Plant	30 MWc	2023	Ministère de l'Energie
Dosso PV Plant	10 MWc	2026	Ministère de l'Energie
Kandadji PV Plant	70 MWc	2026	Ministère de l'Energie
Bangoula PV Plant	70 MWc	2028	Ministère de l'Energie

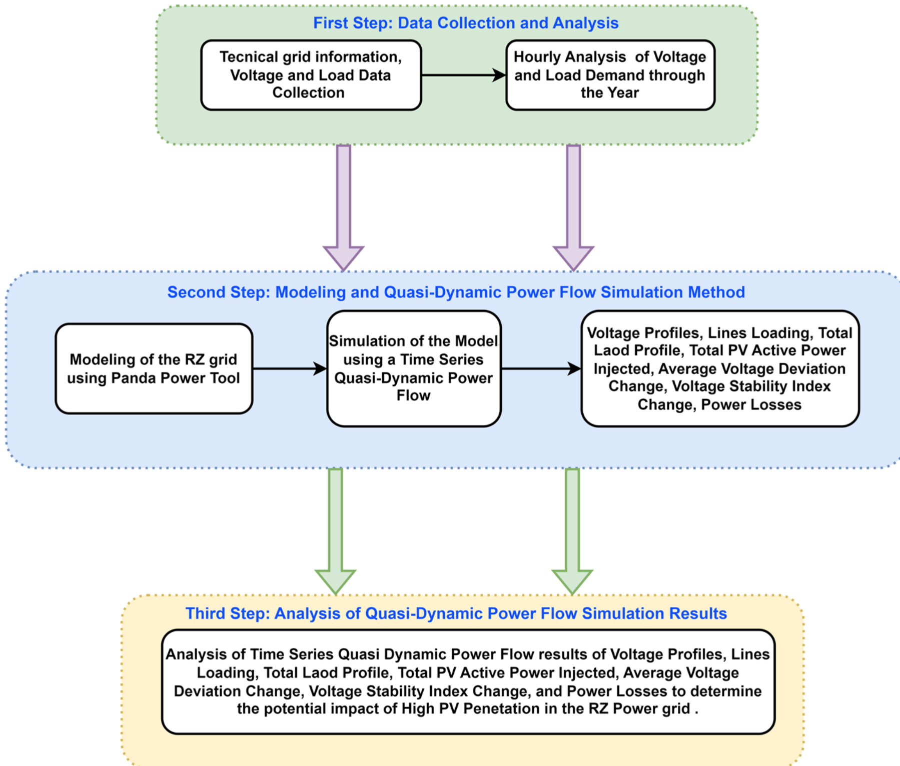

Fig. 3 Methodological framework for voltage stability assessment

using data provided by Niger's electricity transmission grid operators (NIGELEC) ensuring that line parameters, transformer ratings, and voltages accurately reflect actual operating conditions. Key components of the RZ grid include: 1) busbars operating at 132 kV, 66 kV, 33 kV and 20 kV, 2) transmission lines with corresponding line impedances and thermal ratings, 3) transformers interconnecting different voltage levels (40 units), 4) generators (8 static, 15 synchronous) representing conventional and renewable sources, 5) general loads (15 aggregated), switches (65), and shunt compensators (16) and, 6) external grid connection enabling interconnection with adjacent networks. In accordance with NIGELEC?s operational practices, voltage control in the Nigerien transmission network is primarily ensured through shunt capacitor banks, which provide dynamic reactive power compensation. These devices are used to both inject and absorb reactive power depending on system conditions, thereby mitigating voltage deviations caused by fluctuating load PV generation. After constructing the network's topology, we validated the base case model by performing a steady state power flow to ensure no initial constraint violation, such as voltages or line loading outside acceptable limits.

2.3.2 Quasi-dynamic simulation setup

High PV penetration often leads to rapid hourly or sub-hourly variation in generation, making a purely static snapshot analysis insufficient. Therefore, we adopted a quasi-dynamic approach, running time-stepped power flow simulations over a representative 24-hour period (extended to 744 h for a monthly analysis) to capture daily load and PV output fluctuations. This method helps quantify how voltage profiles, line loadings, and stability indices evolve over time.

- Load and PV profiles:

The hourly load curves were derived from historical and forecasted data, while the PV generation profiles were computed from expected solar irradiance patterns in the RZ region.

- Power flow algorithm:

A Newton–Raphson solver [25] was used for each hourly time step, with a convergence tolerance of 1×10^{-6}. Each hour required, on average, 4 iterations to converge, resulting in a total of 2976 power flow solutions for a month-long (744 h) simulation.

- Initial conditions:

The bus voltages were initialized between 0.90 and 1.05 p.u., while the generator active/reactive outputs followed scheduled setpoints. Equations (1) and (2) represent the iterative power flow formulation.

$$P_m = \sum_{k=1}^{N} |V_m||V_k| \left(G_{mk} \cos(\theta_m - \theta_k) + B_{mk} \sin(\theta_m - \theta_k)\right) \tag{1}$$

$$Q_m = \sum_{k=1}^{N} |V_m||V_k| \left(G_{mk} \sin(\theta_m - \theta_k) - B_{mk} \cos(\theta_m - \theta_k)\right) \tag{2}$$

Where, P_m and Q_m are the active and reactive power injections at bus *m*, V_m is the bus voltage magnitude at bus *m*, and G_{mk} and B_{mk} are the conductance and susceptance between buses *m* and *k*.

To comprehensively evaluate grid behavior under varying load and PV generation, we tracked six core performance metrics: voltage profiles, line loading, total load, total PV output, voltage stability indices, and power losses. These metrics are computed at each time step in the quasi-dynamic simulation.

2.3.3 Voltage profile calculation

To ensure acceptable power quality, bus voltages at each time step $t \in [1\,\text{h},\ 744\,\text{h}]$ were computed in per-unit using Eq. (3):

$$V_{pu} = \frac{V_{actual}}{V_{base}} \tag{3}$$

Where, V_{actual} is the bus voltage (kV) and V_{base} is the nominal voltage of the bus (kV). Acceptable Voltage limits were set as:

$$0.90 \leq V_{\text{pu}} \leq 1.05 \tag{4}$$

Any bus with $V_{pu} < 0.90$ or $V_{pu} > 1.05$ was flagged for potential undervoltage or overvoltage issues.

2.3.4 Line loading evaluation

Line loading (LL) ensures each transmission line operates at its thermal capacity, and it is expressed in Eq. (5).

$$\text{Loading}(\%) = \frac{I_{\text{actual}}}{I_{\text{rated}}} \times 100 \tag{5}$$

Where,

$$I_{\text{actual}} = \frac{|S_{\text{actual}}|}{\sqrt{3} \cdot V_{\text{line}}} \tag{6}$$

I_{actual} is derived from the apparent power S_{actual} flowing through the line at voltage V_{line} and I_{rated} is the maximum allowable current. Lines exceeding 100% loading are marked as overloading, signaling a thermal violation that can compromise system reliability [26].

2.3.5 Total load calculation

To monitor how demand varies throughout the day, we sum the active power across all loads using Eq. (7).

$$P_{\text{load,total}}(t) = \sum_{i=1}^{N_{\text{loads}}} P_{\text{load},i}(t) \tag{7}$$

Here $P_{\text{load},i}(t)$ is the active power demand of load i at hour t and N_{loads} is the total number of loads. This metric helps correlate demand peaks with voltage fluctuations or overloading.

2.3.6 Total PV power injection

Similarly, the total PV generation at each time step is tracked in the eq. (8).

$$P_{\text{PV,total}}(t) = \sum_{j=1}^{N_{\text{PV}}} P_{\text{PV},j}(t) \tag{8}$$

Where $P_{\text{PV},j}(t)$ represents the active power outputs of the PV generator j at time t. Comparing $P_{\text{PV},j}(t)$ with $P_{\text{load,total}}(t)$ helps identify times when PV surplus (or deficit) may cause overvoltage or undervoltage.

2.3.7 Voltage stability index (VSI) calculation

Voltage stability is a fundamental aspect of power system security, particularly in networks subject to rising active power demand and increasing penetration of variable renewable energy sources. In this study, we evaluate the proximity of the RZ grid to voltage collapse using a VSI formulation that emphasizes the influence of active power loading. Among the various indices proposed in the literature, including those based on reactive power sensitivity [27, 28] and Thevenin equivalent methods, we adopt a simplified and computationally efficient formulation initially introduced in [29]. This index captures the relationship between the sending bus voltage, the impedance of the interconnecting line, and the active power demand at the receiving bus, allowing for rapid screening of potential weak points across the network[30, 31]. The VSI for a given bus i is defined by Eq.(9):

$$\mathrm{VSI}_i = \frac{|V_i|}{|V_i|^2 - 4Z_{ij}^2 P_j^2} \tag{9}$$

where:

- $|V_i|$ is the voltage magnitude at bus *i*,
- Z_{ij} is the magnitude of the impedance between buses *i* and *j*,
- P_j is the active power demand at bus *j*.

As active power demand increases or line impedance becomes significant, the denominator in Eq. (9) diminishes, causing the VSI to approach zero, an indication of increased susceptibility to voltage instability. This characteristic makes the index particularly well-suited for evaluating scenarios involving load growth, network congestion, or peak-demand stress.

The VSI was applied to the RZ grid using hourly AC power flow simulations. At each time step, the index was computed for all buses in the system. Buses exhibiting VSI values below 0.25 were flagged as critical, in accordance with threshold values suggested in prior studies [32, 33]. Compared to more complex techniques such as modal analysis or continuation power flow, this VSI-based approach provides a transparent, computationally lightweight, and scalable method for identifying voltage stability issues in large-scale time-series assessments.

2.3.8 Voltage deviation and total voltage distortion (TVD)

To quantify how PV integration changes overall grid voltage quality, we track the voltage deviation at each bus i for each time step t as shown in Eq (10):

$$\Delta V_{\mathrm{pu},i}(t) = |V_{\mathrm{pu},i}(t) - 1.0| \tag{10}$$

With, V_{pu} is the per-unit voltage at bus i at time step t. The average deviation across all time steps is given by:

$$\overline{\Delta V_{\mathrm{pu},i}} = \frac{1}{24}\sum_{t=1}^{24} \Delta V_{\mathrm{pu},i}(t) \tag{11}$$

Then, the change in Voltage Deviation due to new PV integration is given by:

$$\Delta\overline{V_{\mathrm{pu},i}} = \overline{\Delta V_{\mathrm{pu},i}}^{\mathrm{Updated}} - \overline{\Delta V_{\mathrm{pu},i}}^{\mathrm{Original}} \tag{12}$$

Where, "Updated" refers to the scenario with PV additions, and "Original" is the reference scenario before PV integration. To capture the grid-wide perspective, the total voltage distortion (TVD) aggregates per-bus deviations is determine using Eq. (13):

$$\mathrm{TVD}(t) = \sum_{i=1}^{N_{\mathrm{buses}}} \Delta V_{\mathrm{pu},i}(t) \tag{13}$$

2.3.9 Power loss calculation

Finally, power losses are computed at each time step by summing the resistive losses in all lines and transformers [34], following a standard nodal formulation in Eq. (14):

$$P_{\text{loss}} = \frac{1}{2} \sum_{t=1}^{24} \sum_{j=1}^{N_B} \sum_{i=1}^{N_B} G_{ij} \left(V_{j,t}^2 + V_{i,t}^2 - 2V_{j,t}V_{i,t}\cos(\theta_{ij,t}) \right) \tag{14}$$

Where, $V_{i,t}$ and $V_{j,t}$ are voltage magnitude of buses i and j at time t, G_{ij} is the conductance of the branches between buses i and j, N_B is the number of buses in the network, and, $\theta_{ij,t}$ is the phase angle between buses i and j at time t.

2.3.10 Voltage control via multi-step capacitor banks

To enhance local voltage stability, reactive power compensation was modelled using dynamically controlled capacitor banks. Each shunt was represented as a discrete set of m identical steps of size Q_{base} Mvar, such that the total injected reactive power at time t is given by[33]:

$$Q_{\text{sh}}(t) = \text{step}(t) \cdot Q_{\text{base}}, \quad \text{step}(t) \in \{0, 1, \ldots, m\} \tag{15}$$

The capacitor steps were activated using a hysteresis-based control scheme:

$$\text{step}(t) = \begin{cases} \text{step}(t-1) + 1, & \text{if } V_i(t) < V_{\text{set}} - \varepsilon \\ \text{step}(t-1) - 1, & \text{if } V_i(t) > V_{\text{set}} + \varepsilon \\ \text{step}(t-1), & \text{otherwise} \end{cases} \tag{16}$$

where $V_i(t)$ is the bus voltage at time t, V_{set} is the reference voltage, and ε is the hysteresis band.

3 Results

3.1 Analysis of load and voltage profile of the river zone grid before PV injection

3.1.1 Load profile

Figure 4 illustrates the hourly power demand for Niamey and Dosso across three critical seasons (each spanning 31 days): January (cold season), May (hot season), and August (rainy season). These profiles underscore the interplay of seasonal and diurnal variations in electricity use within the RZ. In the cold season (January), as shown in Fig. 4a (Niamey) and Fig. 4d (Dosso), both cities exhibit similar diurnal patterns, with morning and

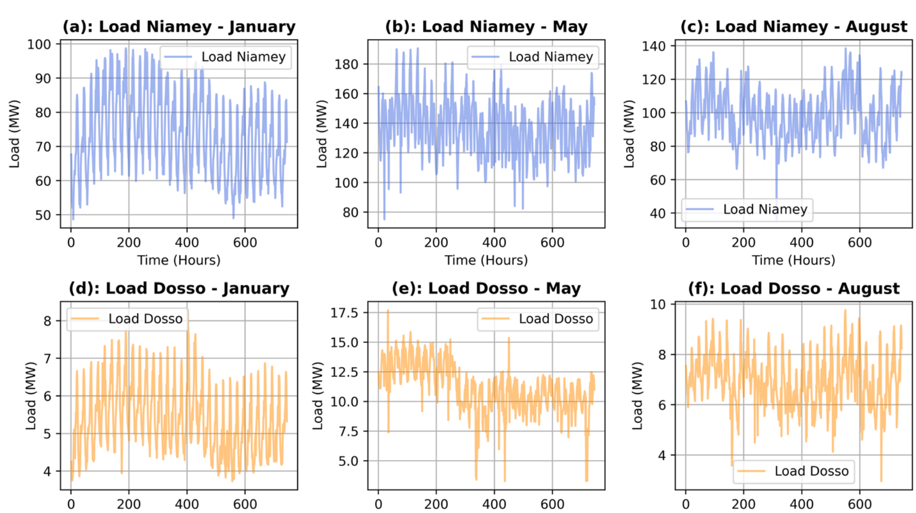

Fig. 4 Daily load profile of the River Zone Grid across the different seasons of the year

evening peaks driven primarily by residential activities such as cooking, lighting, and television usage. Interestingly, a gradual decrease in demand emerges toward the latter part of January. This phenomenon appears linked to rising temperatures, which reduce nighttime energy consumption. These observations align with prior studies, which indicate that warmer evenings can substantially reduce residential demand [35]. During the hot season (May), illustrated in Fig. 4b (Niamey) and Fig. 4e (Dosso), there is a significant increase in power consumption. The most pronounced peaks occur during the daytime, aligning with increased cooling requirements due to high temperatures. Niamey's load level shows a higher magnitude and more pronounced fluctuations than Dosso's, reflecting the city's more substantial commercial and industrial base. Notably, the frequency and intensity of these peaks point to the importance of peak-shaving strategies such as demand response, energy storage, or targeted PV deployment. In the rainy season (August), shown in Fig. 4c (Niamey) and Fig. 4f (Dosso), the load profile generally remains above January levels but drops below May's peaks. The cooling effect of frequent rainfall and cloud coverage moderates the demand for air conditioning, leading to relatively stable consumption patterns throughout the day. While overall demand decreases compared to May, these levels remain higher than January, confirming that multiple factors beyond temperature influence the region's electricity needs. Collectively, these findings reinforce seasonal peak shifting in both Niamey and Dosso: May records the highest system stresses, while August experiences moderate cooling-driven demand reductions. Niamey consistently exhibits greater load magnitude and variability than Dosso, underscoring the city's concentrated residential, commercial, and industrial consumption. These trends align with research linking elevated temperature, increased cooling degree days (CDD), and maximum temperature (Tmax) to higher overall electricity use [36].

3.1.2 Voltage profile

Figure 5 shows the hourly voltage profiles at the Niamey II and Birnin Kebbi (Nigeria) substations over a 744-hour period in January (cold season), May (hot season), and August (rainy season). These results correspond to the base case scenario, i.e., the grid operating prior to any PV injection. They are derived from real operational data

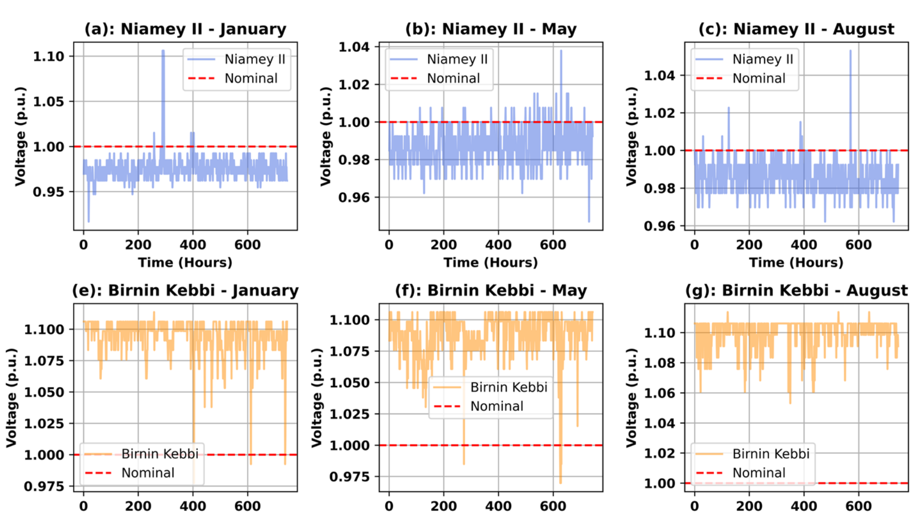

Fig. 5 Daily voltages profiles of the river zone grid across the different seasons

collected from the utility network and serve as the reference benchmark for evaluating existing voltage conditions in the RZ. The nominal voltage is indicated by a red dashed line at 1.0?p.u., while the acceptable operating limits, according to the national grid code, range from 0.90 p.u. to 1.05 p.u. (see Table 3) [37].

At Niamey II, voltage values generally vary between 0.95 p.u. and 1.00 p.u., with occasional drops nearing 0.90 p.u. These dips suggest that local voltage is highly sensitive to demand variations, particularly during consumption peaks or when power imports from Birnin Kebbi fall short of balancing real-time load. Due to Niamey II's strong dependence on external supply, any supply–demand imbalance tends to drive voltages toward the lower operational limit. Conversely, Birnin Kebbi consistently exceeds 1.05 p.u., indicating persistent overvoltage conditions that can propagate through the downstream network. As the primary external supply point for the RZ grid, such high voltage levels may contribute to equipment stress, particularly under high-demand conditions. To address both undervoltage issues at Niamey II and overvoltage at Birnin Kebbi, reinforcement measures such as local generation capacity upgrades, improved load distribution, or voltage regulation mechanisms (e.g., on-load tap changers, capacitor switching) may be required to maintain optimal operational conditions.

3.2 Analysis of Quasi-dynamic simulations in january, may, and august

Figs. 6, 7, and 8 illustrate the simulation results for January, May, and August, respectively, showing the voltage profiles of the main substation buses, line loading levels, total load profiles, and total active power injected by the PV plants.

3.2.1 Analysis of Bus voltage, LL, total load profile, and PV generation in january

The voltage profile in Fig. 6a indicates notable fluctuations at most buses, with some nodes, particularly those connected to PV plants (Gbda_PV_20kV, Bgla_PV_20kV), dropping below 0.9 p.u. during simultaneous peak demand and high PV output. These dips are primarily driven by high active power injection from PV sources during mid-day combined with elevated local demand, which increases current flows and reduces the effective voltage support of lines and transformers. The problem is further exacerbated by the insufficient reactive power compensation provided by NIGELEC?s existing shunt capacitor installations, which were not adequately dispatched to counteract the voltage stress. In addition, PV inverters typically operate at unity power factor, thereby contributing little to local reactive support. Consequently, the lack of effective reactive power control amplifies voltage instability risks during periods of coincident high demand and strong PV generation. By contrast, buses such as Kandadji PV (Kdj_PV_20kV) sustain near nominal voltage, due to robust reactive power support from the Kandadji Dam. This observation aligns with a recent study by [38], highlighting hydropower's crucial role in maintaining grid voltage stability through significant reactive power capability.

Beyond voltage concerns, line loading is another pivotal factor in system reliability. As shown in Fig. 6b, the Birnin Kebbi-Dosso line (L_Bkk_Dso) approaches 140% of its

Table 3 Grid code Regulation of voltage level standards

Bus Voltage	Voltage condition
$> 1.05\,\text{p.u.}$	Overvoltage
$0.90\,\text{p.u.} - 1.05\,\text{p.u.}$	Stable
$< 0.90\,\text{p.u.}$	Undervoltage

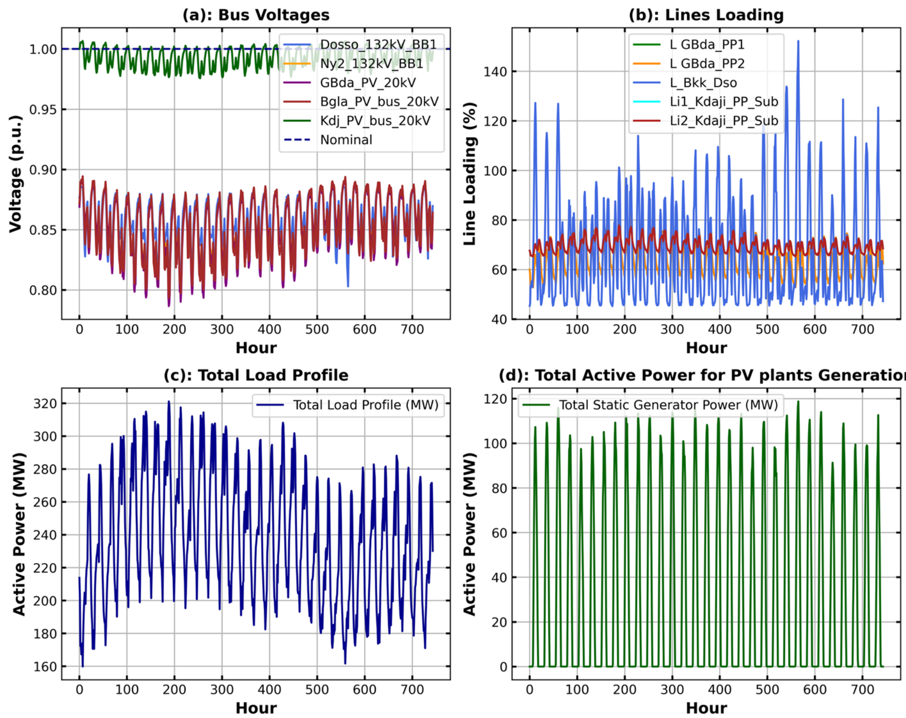

Fig. 6 RZ grid voltage profile, line loading, load profile and PV active power injected in January

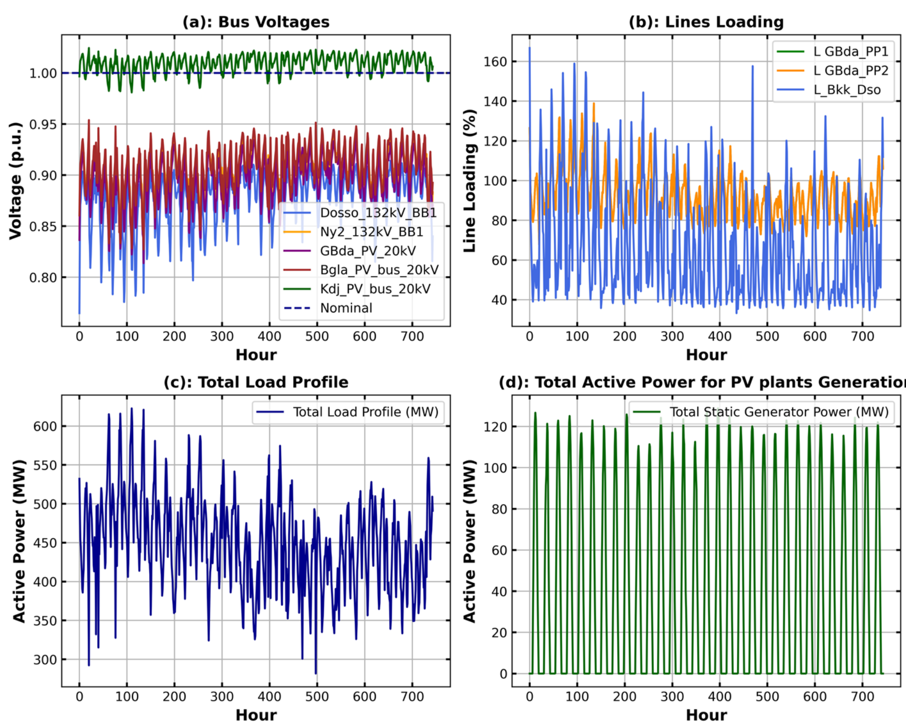

Fig. 7 RZ grid voltage profile, line loading, load profile and PV active power injected in May

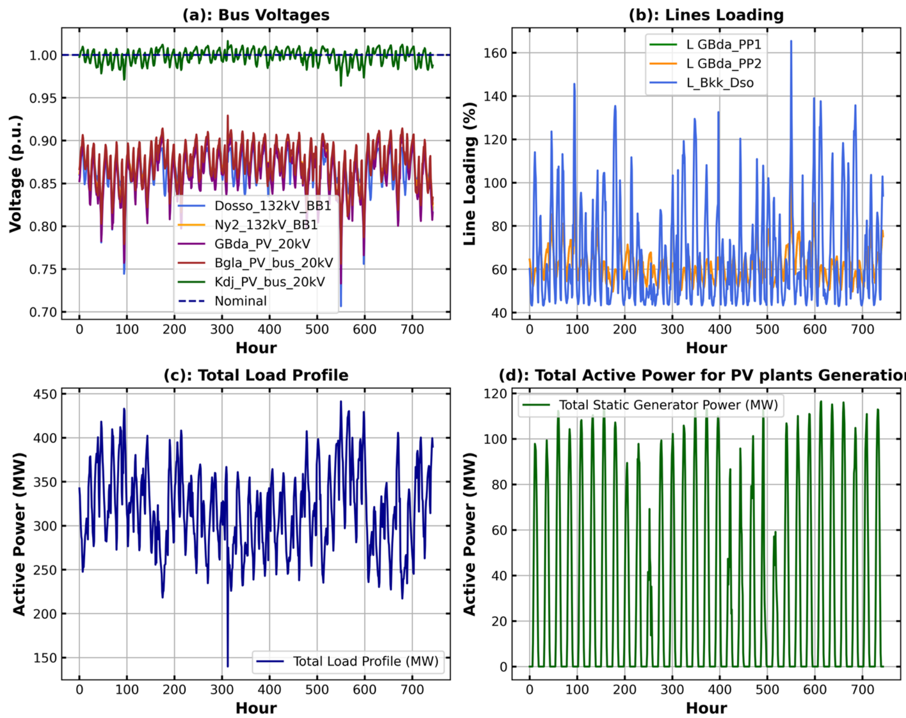

Fig. 8 Grid voltage profile, line loading, load profile and PV active power injected in August

rated capacity during peak demand hours. Such overloading imposes thermal stress on conductors and can trigger protective relay actions, risking line disconnection. [39] highlights that excessive line loading not only accelerates aging but also reduces network security margins, increasing the risk of cascading failures in stressed conditions. These findings justify the identification of line overloads as key indicators of potential reliability degradation.

The total active power demand (Fig. 6c) exhibits a pronounced diurnal pattern, peaking near 320 MW. Coupled with intermittent PV generation, these load swings present balancing challenges and highlight potential risks for voltage and frequency stability during transitions between high and low PV output periods.

Meanwhile, the PV generation profile (Fig. 6d) follows a typical bell-shaped curve, significantly supporting the grid during daylight hours but creating a reliability gap during evening peaks when solar PV output drops. This discrepancy underscores the importance of energy storage and complementary generation, for instance, hydropower or gas turbines, to ensure a more seamless alignment between supply and demand. Overall, the January results reveal that while hydropower support helps stabilize certain buses, the combination of high PV penetration, peak demand, and line constraints necessitates targeted measures ranging from reactive power control to infrastructure reinforcements to maintain both voltage stability and thermal security in the RZ grid.

3.2.2 Analysis of bus voltage, line loading, total load profile, and PV generation in may

Figure 7a reveals substantial voltage dips, in some instances dropping below 0.80 p.u. at PV-connected buses (Gbda_PV_20kV), indicating high sensitivity to load and generation fluctuations. These depressions are primarily caused by the combined effect of peak mid-day PV injection and elevated demand, which increase current flows and accentuate feeder impedance drops. The situation is aggravated by the limited contribution of NIGELEC?s installed shunt capacitor banks, which fail to provide sufficient dynamic reactive power support under rapidly changing operating conditions. In contrast, buses such as Kandadji PV (Kdj_PV_20kV) maintain near-nominal voltages due to substantial reactive power reinforcement from the hydropower station, underlining the importance of local reactive compensation. These disparities emphasize the urgent need for enhanced voltage regulation strategies?such as optimized shunt capacitor dispatch, dynamic reactive power compensation, or advanced inverter control?to mitigate undervoltage risks during coincident peaks of load and PV generation.

Line loading profiles (Fig. 7b) underscore similar concerns, with the Birnin Kebbi?Dosso line frequently exceeding 140% of rated capacity. This severe overloading coincides with peak PV generation and elevated demand typical of May, exposing the network to thermal stress and potential reliability issues. Overloaded lines can experience higher losses, elevated conductor temperatures, and sag risks, all of which compromise grid integrity. Timely reinforcement or optimized dispatch strategies could alleviate these bottlenecks and improve overall system performance.

Meanwhile, the total load profile (Fig. 7c) displays daily peaks approaching 600 MW, driven by heightened residential, commercial, and industrial demand in May. This load surge further strains the grid during daytime peaks, creating a challenging operational window when both demand and PV generation peak. The variability in load and solar output necessitates robust balancing mechanisms to maintain stable voltages and avoid line overloads.

Lastly, the PV generation curve (Fig. 7d) reflects diurnal solar irradiance, providing significant daytime support but no contribution during evening peaks. This reliability gap underscores the need for energy storage or supplementary generation to ensure a smooth supply profile. These findings echo [40], who emphasize the importance of advanced control strategies and power electronic converters in accommodating renewable variability. By adopting these measures alongside grid reinforcements and strategic planning, the RZ network can more effectively integrate rising PV penetration while maintaining stable, efficient operation.

3.2.3 Analysis of bus voltage, line loading, total load profile, and PV generation in august

August is characterized by heavy rainfall in Niger, which has significant implications for both PV output and grid reliability. As shown in Fig. 8a, several PV-connected buses, including Gorou Banda (Gbda_PV_20kV) and Bangoula (Bgla_PV_20kV), experience voltage dips below the acceptable lower limit of 0.9 p.u. These undervoltage events are driven by reduced solar irradiance from cloud cover, which lowers active PV output while simultaneously increasing system stress due to fluctuating load demand. The situation is further exacerbated by the limited contribution of existing shunt capacitor banks, which provide insufficient reactive power support under such variable operating conditions. Consequently, the system becomes more dependent on conventional generation sources and vulnerable to voltage instability during heavy rainfall periods, highlighting the need for enhanced reactive compensation and adaptive control strategies.

Line loading variations (Fig. 8b) also highlight potential bottlenecks. The Birnin Kebbi-Dosso line (L_Bkk_Dso) regularly exceeds 100% capacity, primarily driven by high import demand. Meanwhile, the Gorou Banda line (L_GBda_PP1) experiences overloading during midday peaks, where active power injections from PV coincide with increased local load. Sustained overloading can degrade conductor lifespan and elevate fault risk, making it a legitimate concern for operational reliability. These issues signal the need for targeted network reinforcements, such as conductor upgrades or additional reactive power support, to mitigate thermal stress and ensure secure power delivery.

The total active power demand (Fig. 8c) exhibits less fluctuation compared to January and May due to reduced cooling loads and more stable weather conditions during the rainy season. Although overall demand remains significant, the more uniform consumption pattern suggests that the system could benefit from enhanced coordination of generation resources and storage to handle the remaining peak periods effectively.

Lastly, the PV generation profile (Fig. 8d) mirrors solar irradiation patterns, featuring a diurnal rise and fall that is less pronounced than in drier months. Cloud cover reduces solar output peaks, underscoring the inherent intermittency of PV in rainy climates [41]. This intermittency emphasizes the importance of accurate forecasting and diverse energy mixes, particularly during the wet season, to maintain stable operations. Integrating storage solutions or flexible dispatchable generation can help bridge gaps when PV output is curtailed by unfavorable weather, thereby strengthening overall system reliability.

3.2.4 Voltage deviation and voltage stability index (VSI) Analysis

Figure 9 compares the change in average voltage deviation (Fig. 9a) and the Voltage Stability Index (VSI) (Fig. 9b) across various buses for January, May, and August following PV integration.

In January, the average voltage deviation increases significantly, particularly at PV-connected buses, due to reduced solar output combined with high seasonal demand. This leads to a more pronounced dip in voltage levels, especially at nodes where PV generation is integrated, increasing the risk of instability. In contrast, May exhibits the smallest voltage deviations. Here, strong solar irradiance enables higher PV output that effectively offsets the load, thereby reducing voltage fluctuations and maintaining system equilibrium.

August presents intermediate behavior in terms of voltage deviation. The moderate fluctuations observed during this month result from a seasonal balance: reduced solar irradiance due to intermittent cloud cover is accompanied by slightly lower demand

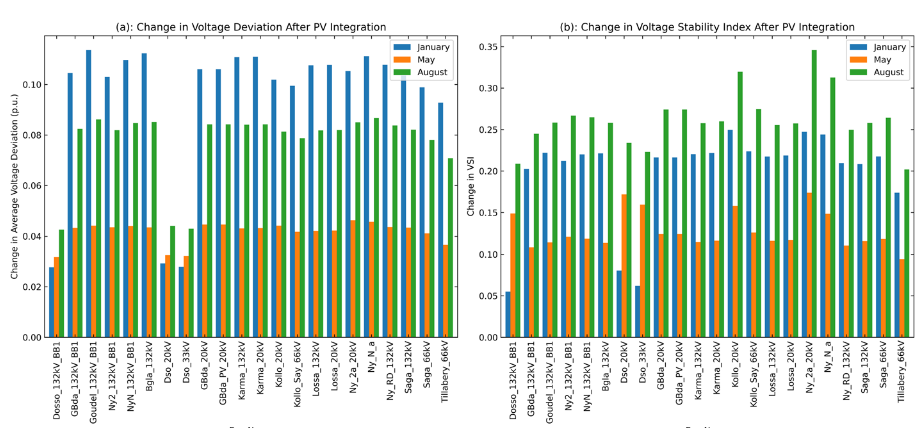

Fig. 9 Change in voltage deviation and VSI after PV integration

resulting from cooler ambient temperatures brought by the rainy season. This results in less extreme mismatches between generation and load, which explains the relatively moderate voltage deviations recorded.

The VSI analysis supports these observations. In May, optimal irradiance conditions ensure minimal VSI variations, reflecting stable operating conditions under high PV generation. In January, VSI values show moderate decline due to low PV penetration and higher dependence on imports and conventional generation. Notably, August displays the most favorable VSI values among the three months, despite PV intermittency. This improved VSI performance is due to more stable reactive power support from conventional generation compensating for the reduced but less volatile PV contribution. Additionally, the flattening of the load profile during rainy periods contributes to more manageable voltage regulation.

This seasonal dynamic underlines the importance of time-resolved analysis when assessing the interplay between PV generation, demand, and voltage stability, particularly in climates with distinct seasonal variability.

3.2.5 Total power losses over time

Figure 10 compares the average hourly power losses in the grid for January, May, and August, illustrating how both demand patterns and PV integration influence overall system efficiency. Each bar in the figure represents the typical hourly losses for a given month, providing a clear view of temporal and seasonal variations. During nighttime and early afternoon hours, the power losses tend to be higher across all three months. In May and August, these peaks are particularly pronounced, reflecting the long-distance power transfers required to meet elevated demand in the absence of adequate local generation. Conversely, the presence of PV during daytime helps to locally offset a portion of the load, reducing the burden on long transmission lines and thereby lowering losses in those hours. Despite these benefits, the grid remains heavily reliant on conventional generation at night, when PV output is unavailable. This reliance leads to increased flows on transmission lines and transformers, contributing to higher overall losses during the late evening and early morning periods. Moreover, seasonal demand plays a critical role. Higher total consumption in May and August results in greater power flows and, consequently, more significant losses. By contrast, January sees comparatively lower demand,

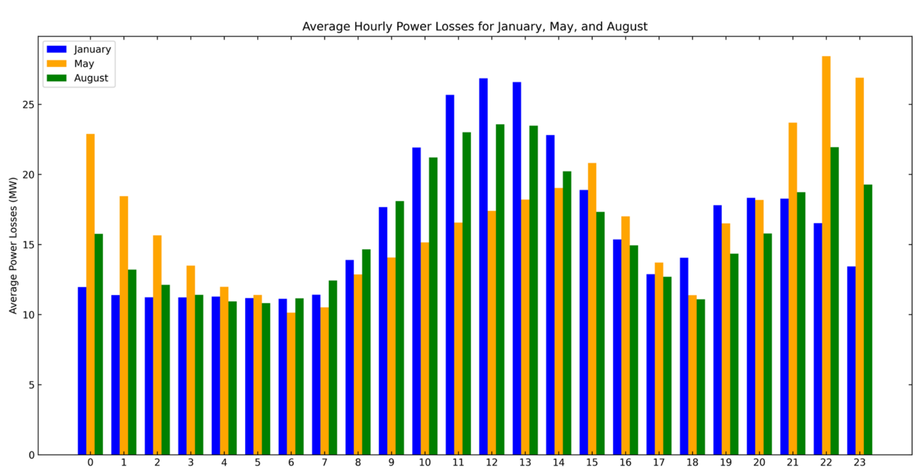

Fig. 10 Total average of Power losses of RZ power grid over time

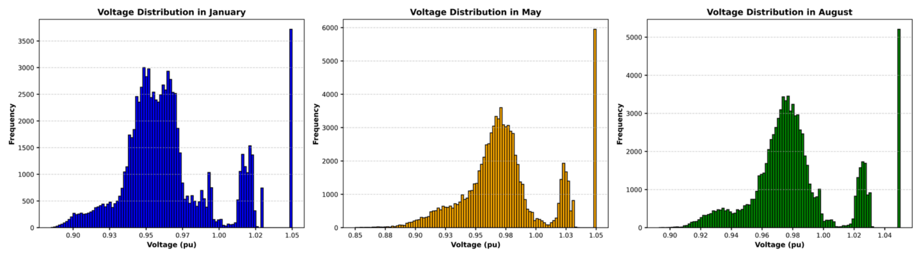

Fig. 11 Voltage distribution with multi-step capacitor banks

although night-time losses can still be substantial when generation is concentrated in specific locations, requiring long-distance transfers. These findings underscore the dual nature of PV integration. While solar generation can improve grid efficiency and reduce losses during daylight hours, night-time and peak periods remain a challenge, often leading to increased reliance on conventional power sources. Addressing these challenges necessitates a holistic approach, including energy storage systems to supply power after sunset, demand side management strategies to shift or reduce peak loads, and advanced grid technologies to optimize power flows. Adopting such measures can help balance load and generation more effectively, thereby mitigating power losses and enhancing overall grid reliability.

3.2.6 Effectiveness of reactive power support via multi-step capacitors

The voltage distribution histograms for January, May, and August after the integration of multi-step capacitor banks are shown in Fig. 11. These results demonstrate the role of reactive power support as a local voltage controller, mitigating fluctuations arising from load variation and PV generation dynamics.

In January, bus voltages are distributed mainly between 0.93 and 1.05 p.u., with a pronounced clustering around 0.95−0.97 p.u. The activation of capacitor banks during peak load hours effectively prevents deeper undervoltage events, which would otherwise cause voltages to drop below 0.90 p.u. threshold. This confirms that the shunt devices provide essential reactive power compensation under stress conditions.

Most voltages lie within 0.95−1.02 p.u. in May, with a reduced frequency of extreme deviations. This highlights the stabilizing effect of the capacitors in balancing both supply- and demand-induced variations, ensuring that buses remain close to nominal values under high load stress and variable PV conditions typical of the hot season.

Finally, in August, the distribution compresses further around 0.96−0.99 p.u. Despite the seasonal variability of demand and PV output during this period, the capacitor banks are observed to offset these dynamics by supplying or absorbing reactive power as required, thereby maintaining the system within the acceptable range of 0.95−1.05 p.u. operational band.

Overall, the results confirm that multi-step capacitor banks serve as effective voltage controllers across different seasonal scenarios. Their deployment narrows the spread of bus voltages, mitigates both under- and overvoltage conditions, and reduces sensitivity to PV generation variability. This highlights the necessity of adequate reactive power support to maintain grid reliability under high renewable energy penetration in the Nigerien context.

4 Discussion

The quasi-dynamic simulations performed in this study highlight the seasonal dynamics of voltage stability in Niger's RZ grid under high PV penetration. In January, significant voltage deviations and moderate VSI declines were observed at PV-connected buses, notably Gbda_PV and Bgla_PV. These instabilities are primarily due to the combined effects of high peak demand and reduced solar output, leading to limited voltage support from PV systems operating at unity power factor. As also reported in [38], the presence of hydropower (e.g., Kandadji Dam) improves voltage profiles through substantial reactive power support, highlighting the importance of hybrid resource integration.

In May, voltage deviation was minimized, and VSI values were more stable, indicating an improved operating regime. This outcome stems from the alignment of high solar generation with elevated daytime demand, which enhances voltage regulation and load balancing-an effect corroborated in similar studies on PV-grid synergy [39]. However, this same period showed the most severe line overloading (e.g., L_Bkk_Dso > 140%), which, as discussed in [39], can reduce system reliability due to thermal stress, accelerated equipment aging, and potential cascading failures.

August exhibited moderate voltage deviation and the best VSI values across the three months. Despite intermittent PV output caused by heavy rainfall and cloud cover [35], demand levels were lower and more stable due to cooler ambient temperatures [35, 38]. The improved VSI in August suggests that even partial PV contributions, when coupled with conventional generation, can maintain sufficient voltage support. This reinforces the importance of diversified generation sources and robust seasonal planning.

A complementary set of simulations incorporating reactive power support via multistep capacitor banks demonstrated the effectiveness of this control strategy in reducing voltage fluctuations. The capacitors narrowed the voltage distributions in all months, particularly preventing deep undervoltage events. In January, capacitor activation during peak load periods avoided drops below 0.90 p.u., while in May and August, voltages were contained within 0.95−1.02 p.u. and 0.96−0.99 p.u., respectively. These results confirm that dynamically controlled shunt compensation provides localized and adaptive voltage support, directly addressing the observed weaknesses of the base case, where existing shunts were insufficient.

These insights provide a foundation for designing adaptive voltage regulation schemes and reinforce the value of time-resolved, data-driven simulation frameworks in planning PV integration in weak or semi-isolated grids.

5 Conclusion

This study provides a comprehensive analysis of the impact of high PV penetration on voltage stability and grid performance in the RZ of Niger. Through time-series quasi-dynamic simulations across three distinct seasonal conditions, January, May, and August, the findings reveal that PV integration, while beneficial in reducing reliance on conventional sources during daylight hours, introduces significant operational challenges. These include voltage instability at PV-connected buses, thermal overloading of key transmission lines, and supply–demand imbalances that are particularly acute during periods of high consumption or reduced solar output. The analysis identifies specific nodes, such as Gbda and Bgla, that are vulnerable to voltage dips, especially during peak load and PV generation periods, while more stable nodes like Kandadji PV benefit from strong reactive power support. The Birnin Kebbi-Dosso line, a critical import corridor, frequently exceeds its rated capacity, particularly in May, which emerges as the most critical month due to high demand and line congestion. August presents intermediate challenges linked to PV intermittency under cloudy conditions, while January highlights the role of limited PV output and cold-season demand in shaping system stress. The study also quantifies the seasonal variation of voltage deviation and VSI, showing that May benefits from balanced generation-load matching, whereas January and August require more active voltage regulation. Furthermore, the effectiveness of reactive power support via multi-step capacitor banks was evaluated. The results demonstrate that their deployment significantly improves bus voltage profiles by narrowing the spread of voltages, mitigating both under- and overvoltage conditions, and reducing sensitivity to PV variability across different seasonal scenarios. In January, capacitor activation prevented deeper undervoltage events below 0.90 p.u., while in May and August, their stabilizing influence maintained most bus voltages within the operational band of $0.95-1.05$ p.u. This confirms their role as essential local voltage controllers that enhance system resilience under high renewable penetration. Based on these results, the study recommends targeted grid reinforcement, improved voltage regulation measures such as capacitor banks and STATCOMs, seasonal planning, and the integration of storage and demand-side management strategies. These interventions are critical for ensuring grid reliability and accommodating increasing shares of solar PV. Future research should examine climatic impacts on PV performance, evaluate decentralized generation and storage options, and explore regulatory implications of high renewable penetration to support Niger's energy transition goals.

Acknowledgements
Our sincere appreciation goes to the Federal Ministry of Education and Research of Germany (BMBF) and West African Science Service Center on Climate Change and Adapted Land Use (WASCAL) for providing the scholarship and financial support for this program.

Author contributions
H.A. and Y.M. conceptualized and designed the study. H.A. conducted the simulation analyses and interpreted the results. A.B. hosted the research visit at his institution, providing critical support and valuable insights throughout the study. H.A. and Y.M. co-wrote the manuscript, while B.A. prepared the figures and assisted with data visualization. M.S. supervised the work and approved the final version. All authors reviewed and approved the final version of the manuscript.

Funding
Hamza Abarchi Halarou received a full scholarship from the German Ministry of Education and Research through the WASCAL program.

Data availability
All Datasets generated and analyzed in this study are available upon reasonable request, with the exception of the hourly input-load data

Declarations

Ethics approval and consent to participate
Not applicable.

Consent for publication
All the authors consent to the submission and publication of this manuscript.

Competing interests
The authors declare that they have no Conflict of interest.

Received: 14 April 2025 / Accepted: 17 January 2026
Published online: 13 February 2026

References

1. Sultan HM, Diab AAZ, Kuznetsov ON, Ali ZM, Abdalla O. Evaluation of the impact of high penetration levels of pv power plants on the capacity, frequency and voltage stability of egypt's unified grid. Energies. 2019. https://doi.org/10.3390/en12030552.
2. Amankwahadu J, Berizzi A, Conte F, D'Agostino F, Ilea V, Napolitano F, et al. Power system stability analysis of the sicilian network in the 2050 osmose project scenario. Energies. 2022. https://doi.org/10.3390/en15103517.
3. Dajuma A, Yahaya S, Touré S, Diedhou A, Konaré RAA, Sido M, et al. Sensitivity of solar photovoltaic panel efficiency to weather and dust over west africa: Comparative experimental study between niamey (niger) and abidjan (côte d'ivoire). Comput Water Energy Environ Eng. 2016. https://doi.org/10.4236/cweee.2016.54012.
4. Halarou, H.A., Bonkaney, A.L., Abdourahimoun, D., Moumouni, Y., Madougou, S.: Application of a long-range energy alternatives planning system to assess electricity supply and demand in niger. In: 2024 International Conference on Green Energy, Computing and Sustainable Technology (GECOST), pp. 217– 223 (2024). https://doi.org/10.1109/GECOST60902.2024.10475120 . https://ieeexplore.ieee.org/document/10475120 Accessed 27 Sep 2024
5. Pouye, M., Moumouni, Y.: A system dynamic model of a distributed generation for energy security in niamey. In: 2018 Advances in Science and Engineering Technology International Conferences (ASET), pp. 1– 5 (2018). https://doi.org/10.1109/ICASET.2018.8376779 . https://ieeexplore.ieee.org/abstract/document/8376779 Accessed 27 Sep 2024
6. Blaabjerg, F., Sangwongwanich, A., Yang, Y.: Chapter 6 - flexible power control of photovoltaic systems. In: Yahyaoui, I. (ed.) Advances in Renewable Energies and Power Technologies, pp. 207– 229. Elsevier, ??? (2018). https://doi.org/10.1016/B978-0-12-812959-3.00006-X . https://www.sciencedirect.com/science/article/pii/B978012812959300006X Accessed 27 Sep 2024
7. Mokred S, Wang Y. Voltage stability assessment and contingency ranking in power systems based on modern stability assessment index. Results Eng. 2024;23:102548. https://doi.org/10.1016/j.rineng.2024.102548
8. Kyeremeh F, Fang Z, Liu F, Peprah F. Techno-economic analysis of reactive power management in a solar pv microgrid: A case study of sunyani to becheam mv feeder, ghana. Energy Rep. 2024;11:83–96. https://doi.org/10.1016/j.egyr.2023.11.031
9. Lu, Z., Li, H., Qiao, Y., Xie, L., Singh, C.: Chapter 14 - deployment and allocation of storage based on flexibility theory. In: Lu, Z., Li, H., Qiao, Y., Xie, L., Singh, C. (eds.) Power System Flexibility, pp. 193– 210. Academic Press, ??? (2024). https://doi.org/10.1016/B978-0-323-99517-7.00019-1 . https://www.sciencedirect.com/science/article/pii/B9780323995177000191 Accessed 29 Sep 2024
10. Munkhchuluun E, Meegahapola L, Vahidnia A. Long-term voltage stability with large-scale solar-photovoltaic (pv) generation. Int J Electr Power Energy Syst. 2020;117:105663. https://doi.org/10.1016/j.ijepes.2019.105663
11. Denholm P, Arent DJ, Baldwin SF, Bilello DE, Brinkman GL, Cochran JM, et al. The challenges of achieving a 100% renewable electricity system in the united states. Joule. 2021;5(6):1331–52. https://doi.org/10.1016/j.joule.2021.03.028.
12. Johlas H, Witherby S, Doyle JR. Storage requirements for high grid penetration of wind and solar power for the miso region of north america: A case study. Renew Energy. 2020;146:1315–24. https://doi.org/10.1016/j.renene.2019.07.043
13. Majeed NI. Nwulu: Reverse power flow due to solar photovoltaic in the low voltage network. IEEE Access. 2023;11:44741–58. https://doi.org/10.1109/ACCESS.2023.3273483
14. Sharma V, Aziz SM, Haque MH, Kauschke T. Effects of high solar photovoltaic penetration on distribution feeders and the economic impact. Renew Sustain Energy Rev. 2020;131:110021. https://doi.org/10.1016/j.rser.2020.110021
15. Cabrera-Tobar A, Bullich-Massagué E, Aragüés-Peñalba M, Gomis-Bellmunt O. Review of advanced grid requirements for the integration of large scale photovoltaic power plants in the transmission system. Renew Sustain Energy Rev. 2016;62:971–87. https://doi.org/10.1016/j.rser.2016.05.044.
16. Salah Saidi A. Impact of grid-tied photovoltaic systems on voltage stability of tunisian distribution networks using dynamic reactive power control. Ain Shams Eng J. 2022;13(2):101537. https://doi.org/10.1016/j.asej.2021.06.023.
17. Alwez MA, Jasni J, MohdRadzi MA, Azis N. Adaptive reactive power control for voltage rise mitigation on distribution network with high photovoltaic penetration. Renew Sustain Energy Rev. 2024;207:114948. https://doi.org/10.1016/j.rser.2024.114948
18. Loutan, C., Klauer, P., Chowdhury, S., Hall, S., Morjaria, M., Chadliev, V., Milam, N., Milan, C., Gevorgian, V.: Demonstration of essential reliability services by a 300 mw solar photovoltaic power plant. Technical Report NREL/TP–5D00-67799, 1349211, National Renewable Energy Laboratory (mar 2017). Publisher: NREL. http://www.osti.gov/servlets/purl/1349211/ Accessed 30 Sep 2024
19. Niger, A.: PRESENTATION DU SYSTEME ELECTRIQUE DU NIGER. Technical report, Autorité de Régulation du Secteur de l'Energie(ARSE) (2020). Publisher: ARSE Niger. https://www.arse.ne/wp-content/uploads/2022/03/PRESENTATION-DU-SYSTEME-ELECTRIQUE.pdf Accessed 8 Oct 2024
20. Power Africa: Off-Grid Solar Market Assessment for Niger. Technical report, U.S Agency for International Development (USAID) (oct 2019). Publisher: U.S Agency for International Development. https://www.usaid.gov/sites/default/files/2022-05/PAOP-Niger-MarketAssessment-Final_508.pdf Accessed 8 Oct 2024
21. Nodalis: PRÉPARATION D'UN PROJET PV AU NIGER: Rapport d'étape 1. Technical report, Agence Française de Développement, Niamey, Niger (2016). https://nodalis.fr/nodalis-niger-centrale-photovoltaique/
22. DESSERT TO Power: Desert-to-Power Roadmap for Niger. Technical report, African Development Bank (oct 2020). Publisher: BAD. https://www.afdb.org/sites/default/files/2024/08/23/desert-to-power_dtp_roadmap_for_niger_en_oct2020.pdf Accessed 8 Oct 2024
23. Thurner L, Scheidler A, Schäfer F, Menke J, Dollichon J, Meier F, et al. pandapower - an open-source python tool for convenient modeling, analysis, and optimization of electric power systems. IEEE Trans Power Syst. 2018;33(6):6510–21. https://doi.org/10.1109/TPWRS.2018.2829021.
24. Alexander Scheidler, Leon Thurner, Markus Kraiczy, Martin Braun: Automated Grid Planning for Distribution Grids with Increasing PV Penetration. In: Workshop Proceeding: 6th International Workshop on Integration of Solar Power Systems, Vienna, Austria (2016). Semantic Scholar. https://www.semanticscholar.org/paper/Automated-Grid-Planning-for-Distribution-Grids-with-Scheidler/47cf7bb7311d740439cdb1528387d215030f20bb Accessed 8 Oct 2024
25. Kundur, P.S., Malik, O.P.: Power System Stability and Control, 2nd edition edn. McGraw-Hill Education, ??? (2022). https://www.accessengineeringlibrary.com/content/book/9781260473544 Accessed 1 Jan 2025

26. Guide, I.: IEEE Guide for Protection Systems of Transmission-to-Generation Interconnections. IEEE Std C37.246-2017 (2018) https://doi.org/10.1109/IEEESTD.2018.8358851 . Conference Name: IEEE Std C37.246-2017. Accessed 11 Oct 2024
27. Musirin, M., Rahman, T.K.A.: Novel fast voltage stability index (fvsi) for voltage stability analysis in power transmission system. In: IEEE Student Conference on Research and Development, pp. 265– 268 (2002). https://doi.org/10.1109/SCORED.2002.1033108
28. Rao AN, Vijaya P, M K. Voltage stability indices for stability assessment: a review. Int J Ambient Energy. 2021;42(7):829–45. https://doi.org/10.1080/01430750.2018.1525585.
29. Moghavvemi M, Faruque M. Power system security and voltage collapse: a line outage based indicator for prediction. Int J Electr Power Energy Syst. 1999;21(6):455–61. https://doi.org/10.1016/S0142-0615(99)00007-1.
30. Kanojia SS, Suthar BN. Voltage stability index: a review based on analytical method, formulation and comparison in renewable dominated power system. Int J Appl. 2024;13(2):508–20. https://doi.org/10.11591/ijape.v13.i2.pp508-520.
31. Asmah, M.W.: Grid integration of variable renewable energies in ghana: Assessment of the impact on system stability. PhD thesis, Doctoral dissertation, TU Dortmund University (2023). https://doi.org/10.17877/DE290R-23887
32. Gao B, Morison G, Kundur P. Voltage stability evaluation using modal analysis. IEEE Trans Power Syst. 2002;7(4):1529–42. https://doi.org/10.1109/59.207377.
33. Mustafa MW, Wong YC. Optimal placement of static var compensator using genetic algorithms. Elektrika J Electr Eng. 2008;10(1):26–31.
34. Putra JT, Sarjiya Setyonegoro MIB. Modeling of high uncertainty photovoltaic generation in quasi dynamic power flow on distribution systems: A case study in java island. Indones Results Eng. 2024;21:101747. https://doi.org/10.1016/J.RINENG.2023.101747
35. Bonkaney A, Madougou S, Adamou R. Impacts of cloud cover and dust on the performance of photovoltaic module in Niamey. J Renew Energy. 2017(1):9107502
36. Bonkaney AL, Abiodun BJ, Sanda IS, Balogun AA. Potential impact of global warming on electricity demand in Niger. Clim Change. 2023;176(4):35. https://doi.org/10.1007/s10584-023-03513-4.
37. Niger, A.: RECUEIL DES TEXTES REGISSANT LA REGULATION ET LE SECTEUR DE L'ENERGIE AU NIGER. Technical report, CABINET DU PREMIER MINISTRE, AUTORITE DE REGULATION DU SECTEUR DE L'ENERGIE, Niamey (may 2024). https://www.arse.ne/wp-content/uploads/2024/05/Recueil-des-textes-de-la-regulation.pdf Accessed 2 Nov 2024
38. Somani, A., Datta, S., Kincic, S., Chalishazar, V.H., Vyakaranam, B.G., Samaan, N.A., Colotelo, A.H., Zhang, Y., Koritarov, V., McJunkin, T.: Hydropower's contributions to grid reliability and resilience. Technical report, Pacific Northwest National Lab. (PNNL), Richland, WA (United States); Argonne (2021). https://www.pnnl.gov/main/publications/external/technical_reports/PNNL-30554.pdf
39. Zainuddin NM, Rahman MA, Kadir MA, Ali NN, Ali Z, Osman M, et al. Review of thermal stress and condition monitoring technologies for overhead transmission lines: Issues and challenges. IEEE Access. 2020;8:120053–81. https://doi.org/10.1109/ACCESS.2020.3004578
40. Blaabjerg F, Yang Y, Yang D, Wang X. Distributed Power-Generation Systems and Protection. Proc IEEE. 2017;105:1–21. https://doi.org/10.1109/JPROC.2017.2696878.
41. Chakraborty D, Mondal J, Barua HB, Bhattacharjee A. Computational solar energy-Ensemble learning methods for prediction of solar power generation based on meteorological parameters in Eastern India. Renew Energy Focus. 2023;44:277–94. https://doi.org/10.1016/j.ref.2023.01.006. (**ISBN: 1755-0084**).

Publisher's Note